Towards Real-Time Maneuver Detection: Automatic State and Dynamics Estimation with the Adaptive Optimal Control Based Estimator

Daniel P. Lubey and Daniel J. Scheeres
University of Colorado, Boulder, United States

ABSTRACT

While an incredible amount of observations of Earth-orbiting objects are taken every day world wide, the actual number of correlated observations for a single object can be quite small. The sheer number of observations precludes human involvement in the processing of each one, but the automated algorithms need to be designed to be robust to data-sparse observations as well as the mismodeled dynamics that are present when observing unidentified objects. This paper presents the Optimal Control Based Estimator, which is a state estimator that simultaneously estimates optimal control policies to represent mismodeled dynamics. The control estimates may be used to detect and reconstruct mismodeled dynamics. This paper details the solution to this nonlinear estimation problem, the associated maneuver detection method, and how the algorithm is automated via the maneuver detection results. A sample tracking application where a spacecraft in GEO undergoes unknown stationkeeping maneuvers demonstrates this algorithm in action. The results show the algorithm's ability to differentiate between data outliers and true maneuvers as well as accurately reconstruct those maneuvers in a completely automated fashion.

1. INTRODUCTION

Tracking objects in Earth orbit is fraught with complications introduced by a large population from increased launching and debris accumulation, passive (i.e. no direct communication) and data-sparse observation, and the presence of maneuvers and dynamics mismodeling. Accurate orbit determination in this environment requires an algorithm to capture both a system's state and its state dynamics in order to account for mismodelings. Previous studies by the authors in this field yielded an algorithm called the Optimal Control Based Estimator (OCBE) - an algorithm that simultaneously estimates a system's state and optimal control policies that represent dynamic mismodeling in the system for an arbitrary orbit-observer setup. The stochastic properties of these estimated controls are then used to determine the presence of mismodelings (maneuver detection), as well as characterize and reconstruct the mismodelings. This paper develops the OCBE into an accurate real-time orbit tracking and maneuver detection algorithm by making it into a nonlinear adaptive estimator.

The OCBE is intended to address estimation in dynamically mismodeled systems, with an emphasis toward mismodeling identification (i.e. maneuver detection) and estimation of the mismodeling (i.e. maneuver reconstruction). Beyond typical methods for dealing with dynamically mismodeled system like process noise and Gauss-Markov processes [11,16,21], there are many methods for dealing with mismodeled dynamics. Input estimation techniques [2,4,7] append control estimates to the state when a maneuver is detected through residuals, however these methods are generally more applicable to highly dynamical systems with a lot of information. SSA focused methods [6, 9, 15, 20] are well adapted problems within the SSA community, but often they are limited in application to specific orbit and/or observation types. Many methods in the field of system identification focus on understanding the dynamics of an unknown system, but most methods require control of the observed system and data-rich measurement sets [1, 5, 17]. Other methods within system identification [3,22] lift these limitations, but they are often designed for specific systems that do not have overlap with SSA problems. Multiple model estimation methods [8, 14] offer yet another approach to this problem, but these methods limit mismodeling to a finite number of models and the complexity of these methods may limit automated implementation. The OCBE is designed to fit the existing hole in the literature - an estimation method that is robust to mismodeling and provides information of mismodeling, works for general systems and observation types, may be automated for real-time implementation, and works well in systems with data-sparse and non-cooperative observation.

In its previous form [19] the OCBE was a linear algorithm that had a parameter called the assumed dynamic uncertainty that had to be selected by the user with each new measurement to reflect the level of dynamic mismodeling in the system. This human-in-the-loop approach precludes real-time application to orbit tracking problems because, though orbit tracking is often data-sparse for a single target, the sheer number of objects in orbit creates a large amount of observations (often uncorrelated) to make the problem quite complex. The authors developed a linear version of an adaptive algorithm that showed promise at providing real-time detection performance [19]. This paper focuses on turning this linear adaptive estimator into a nonlinear adaptive estimator, and applying this algorithm to a sample tracking application.

Section II of this paper will focus on defining the OCBE. This includes its nonlinear definition, and a definition of a linear form of it that may be iterated to converge on the nonlinear solution. Section III focuses on the maneuver detection and reconstruction properties of the estimator, and how these may be leveraged to automate the algorithm. Section IV provides a sample tracking application where the OCBE is used to detect and reconstruct maneuvers of a GEO spacecraft. Finally, Section V provides a concluding discussion summarizing the important aspects of the OCBE as well as directions for future progress in this research.

2. THE OPTIMAL CONTROL BASED ESTIMATOR

The OCBE is a unique estimator that models mismodeled dynamics as an optimal control process. These controls may be used to detect the presence of mismodeling as well as identify its source. In this section we will define the nonlinear algorithm, and a linearized version that may be iterated to solve the nonlinear optimization problem.

2.1. Nonlinear OCBE

The OCBE is defined as the estimator that minimizes the cost function in Eq. 1 constrained such that the state dynamics are of the form: $\dot{\vec{x}}(t) = f(t,\vec{x}) + B(t)\vec{u}(t)$. In this definition the inputs are as follows: the a priori epoch (t_{k-1}), the a priori state estimate ($\bar{x}_{k-1|k-1}$) and its covariance ($\bar{P}_{k-1|k-1}$), the measurement epoch (t_k), the measurement ($\vec{Y}_k$) and its covariance (R_k), the observation-state relationship ($h(t,\vec{x})$), and the a priori mismodeling estimate ($\bar{u}(t)$) and its covariance ($\tilde{Q}(t)$).

$$\begin{aligned}\mathcal{J}\left(\vec{x}_{k-1},\vec{x}_k,\vec{u}(t)\right) =& \frac{1}{2}\left(\bar{x}_{k-1|k-1}-\vec{x}_{k-1}\right)^T \bar{P}^{-1}_{k-1|k-1}\left(\bar{x}_{k-1|k-1}-\vec{x}_{k-1}\right) \\ &+ \frac{1}{2}\left(\vec{Y}_k - h(t_k,\vec{x}_k)\right)^T R_k^{-1}\left(\vec{Y}_k - h(t_k,\vec{x}_k)\right) \\ &+ \int_{t_{k-1}}^{t_k} \frac{1}{2}\left(\vec{u}(t)-\bar{u}(t)\right)^T \tilde{Q}(t)^{-1}\left(\vec{u}(t)-\bar{u}(t)\right) d\tau\end{aligned} \tag{1}$$

Applying functional optimization methods as discussed by Lawden [12, 13], the set of necessary conditions for optimality are obtained as defined in Eqs. 2-5.

$$\vec{F}_1(\hat{x}_{k-1|k},\hat{x}_{k|k},\hat{p}_{k-1|k}) = \phi_p(t_k;t_{k-1},\hat{x}_{k-1|k},\hat{p}_{k-1|k}) + \left.\frac{\partial h}{\partial \vec{x}_k}\right|^T_{(t_k,\hat{x}_{k|k})} R_k^{-1}\left(\vec{Y}_k - h(t_k,\hat{x}_{k|k})\right) = \vec{0} \tag{2}$$

$$\vec{F}_2(\hat{x}_{k-1|k},\hat{x}_{k|k},\hat{p}_{k-1|k}) = \hat{p}_{k-1|k} - \bar{P}^{-1}_{k-1|k-1}\left(\bar{x}_{k-1|k-1}-\hat{x}_{k-1|k}\right) = \vec{0} \tag{3}$$

$$\vec{F}_3(\hat{x}_{k-1|k},\hat{x}_{k|k},\hat{p}_{k-1|k}) = \hat{x}_{k|k} - \phi_x(t_k;t_{k-1},\hat{x}_{k-1|k},\hat{p}_{k-1|k}) = \vec{0} \tag{4}$$

The goal is to estimate the state at the a priori epoch ($\hat{x}_{k-1|k}$), state at the measurement epoch ($\hat{x}_{k|k}$), and adjoint at the a priori epoch ($\hat{p}_{k-1|k}$) such that all three equations are satisfied ($\phi_x(t)$ and $\phi_p(t)$ represent state and adjoint solution flows, respectively). The adjoint is the Lagrange multiplier that enforces the state dynamical constraint. It relates to the estimated optimal control policy through the results of the Pontryagin Minimum Principle (Eq. 5), and it has dynamics given by Eq. 6.

$$\hat{u}(t) = -\tilde{Q}(t)B(t)^T\hat{p}(t) + \bar{u}(t) \tag{5}$$

$$\dot{\hat{p}}(t) = -\left.\frac{\partial f}{\partial \vec{x}}\right|^{T}_{(t,\hat{x}(t))} \hat{p}(t) \tag{6}$$

This estimator has no analytical solution for a nonlinear system. We desire a method to solve the necessary conditions to estimate the state and control trajectories. This is accomplished via a linearization of the necessary conditions, which results in an algorithm called the Generalized Linear OCBE (GL-OCBE).

2.2. Generalized Linear OCBE

The GL-OCBE is a version of the OCBE, which is linearized about arbitrary initial state and adjoint values ($\tilde{x}_{k-1}$ and $\tilde{p}_{k-1}$). The nominal state and adjoint trajectories are defined as the expectations of the solution flows that evolve from these initial conditions ($\tilde{x}(t) = E\left[\phi_x(t; t_{k-1}, \tilde{x}_{k-1}, \tilde{p}_{k-1})\right]$ and $\tilde{p}(t) = E\left[\phi_p(t; t_{k-1}, \tilde{x}_{k-1}, \tilde{p}_{k-1})\right]$). Accompanying this linearization are linearized versions of the measurement, a priori state estimate, and the state-observation relationship as defined in Eqs. 7-9. The state transition matrix (STM), which includes both the state and adjoint linear dynamics ($\phi(t) = \left[\begin{array}{cc} \phi_x(t)^T & \phi_p(t)^T \end{array}\right]^T$), is defined in Eq. 10.

$$\delta\vec{y}_k = \vec{Y}_k - h(t_k, \tilde{x}_k) \tag{7}$$

$$\delta\bar{x}_{k-1|k-1} = \bar{x}_{k-1|k-1} - \tilde{x}_{k-1} \tag{8}$$

$$\tilde{H}_k = \left.\frac{\partial h}{\partial \vec{x}}\right|_{(t_k,\tilde{x}_k)} \tag{9}$$

$$\Phi(t,\tau) = \frac{\partial \phi(t)}{\partial \phi(\tau)} = \left[\begin{array}{cc} \Phi_{xx}(t,\tau) & \Phi_{xp}(t,\tau) \\ \Phi_{px}(t,\tau) & \Phi_{pp}(t,\tau) \end{array}\right] \tag{10}$$

The GL-OCBE also explicitly accounts for the effects of process noise via the state and adjoint process noise terms defined in Eqs. 11. In this definition $\vec{w}(t)$ is the stochastic component of $\bar{u}(t)$ such that it has the following properties: $E\left[\vec{w}(t)\right] = 0$ and $E\left[\vec{w}(t)\vec{w}(\tau)^T\right] = \tilde{Q}(t)\delta(t-\tau)$.

$$\begin{aligned} \vec{v}_x(t|t_{k-1}) &= \int_{t_{k-1}}^{t} \Phi_{xx}(t,\tau)B(\tau)\vec{w}(\tau)d\tau \\ \vec{v}_p(t|t_{k-1}) &= \int_{t_{k-1}}^{t} \Phi_{px}(t,\tau)B(\tau)\vec{w}(\tau)d\tau \end{aligned} \tag{11}$$

After linearizing and simplifying the results, the GL-OCBE equations are obtained in a Kalman Filter-like formulation. First we start with the time update equations defined below.

$$\delta\bar{x}_{k|k-1} = \left(\Phi_{xx} + \mathcal{P}_{k|k-1}\Phi_{px}\right)\delta\bar{x}_{k-1|k-1} \tag{12}$$

$$\mathcal{P}_{k|k-1} = \left(\Phi_{xx}\bar{P}_{k-1|k-1} - \Phi_{xp}\right)\left(\Phi_{pp} - \Phi_{px}\bar{P}_{k-1|k-1}\right)^{-1} \tag{13}$$

$$\begin{aligned} \dot{\bar{P}}(t|t_{k-1}) = &\left[A_{xx}(t) + \mathcal{P}(t|t_{k-1})A_{px}(t)\right]\bar{P}(t|t_{k-1}) + \bar{P}(t|t_{k-1})\left[A_{xx}(t) + A_{px}(t)\mathcal{P}(t|t_{k-1})\right]^T \\ &+ B(t)\tilde{Q}(t)B(t)^T \end{aligned} \tag{14}$$

These equations propagate information form the a priori epoch to the measurement epoch in a manner similar to a Kalman Filter. In terms of notation, $\delta\bar{x}_{k|k-1}$ is the propagated a priori state, $\mathcal{P}_{k|k-1}$ is the propagated a priori state quasi-covariance, and $\bar{P}_{k|k-1}$ is the propagated a priori state covariance.

The measurement update is broken up into three portions corresponding to the three estimates. First, the state estimate at the measurement epoch is defined in Eqs. 15-17.

$$\delta\hat{x}_{k|k} = \left(\delta\bar{x}_{k|k-1} + \tilde{b}_k + \vec{v}_x(t_k)\right) + L_k\left[\delta\vec{y}_k - \tilde{H}_k\left(\delta\bar{x}_{k|k-1} + \tilde{b}_k + \vec{v}_x(t_k)\right)\right] \tag{15}$$

$$L_k = \mathcal{P}_{k|k-1}\tilde{H}_k^T\left(R_k + \tilde{H}_k\mathcal{P}_{k|k-1}\tilde{H}_k^T\right)^{-1} \tag{16}$$

$$\tilde{b}_k = \mathcal{P}_{k|k-1}\left(\tilde{p}_k + \vec{v}_p(t_k|t_{k-1})\right) - \left(\Phi_{xx} + \mathcal{P}_{k|k-1}\Phi_{px}\right)\bar{P}_{k-1|k-1}\tilde{p}_{k-1} \tag{17}$$

The biasing term ($\tilde{b}_k$) helps to account for the presence of the non-ballistic trajectory (i.e. a nonzero nominal adjoint trajectory). Analyzing these equations, we conclude that it is unbiased, and it has a form very similar to the Kalman Filter other than the presence of the adjoints. It can be shown that for a ballistic nominal trajectory the GL-OCBE state estimate at the measurement epoch is fully equivalent to the Kalman estimate [18].

Next, the state estimate at the a priori epoch is defined in Eqs. 18-21.

$$\delta\hat{x}_{k-1|k} = \mathcal{I}_{k-1}\left(\delta\bar{x}_{k-1|k-1} + \tilde{b}_{k-1}\right) + L_{k-1}\left[\delta\vec{y}_k - \tilde{H}_k\left(\delta\bar{x}_{k|k-1} + \tilde{b}_k + \vec{v}_x(t_k|t_{k-1})\right)\right] \tag{18}$$

$$\mathcal{I}_{k-1} = I_{n\times n} + \bar{P}_{k-1|k-1}\left(\Phi_{pp} - \Phi_{px}\bar{P}_{k-1|k-1}\right)^{-1}\Phi_{px} \tag{19}$$

$$L_{k-1} = \left(\Phi_{pp}\bar{P}^{-1}_{k-1|k-1} - \Phi_{px}\right)^{-1}\tilde{H}_k^T\left(R_k + \tilde{H}_k\mathcal{P}_{k|k-1}\tilde{H}_k^T\right)^{-1} \tag{20}$$

$$\tilde{b}_{k-1} = \bar{P}_{k-1|k-1}\left[\Phi_{pp}^{-1}\left(\tilde{p}_k + \vec{v}_p(t_k|t_{k-1})\right) - \tilde{p}_{k-1}\right] \tag{21}$$

Again, analysis leads to the result that the estimate is unbiased. It can be shown that this results in the assumption that the a priori and measurement epoch true states are ballistically connected. This makes sense based on the form of the OCBE cost function, which penalizes any deviation from the a priori mismodeling estimate. Furthermore, it can be shown that when the nominal trajectory is ballistic this estimate is equivalent to a smoothed Kalman estimate [18]. Combining this with properties of the measurement epoch estimate, it can be shown that the OCBE linearized about a ballistic nominal trajectory is a generalization of the Kalman algorithm. This version of the OCBE is called the Ballistic Linear OCBE (BL-OCBE).

The third and final piece of information is the adjoint estimate at the a priori epoch (Eq. 22). This estimate indicates that the nonlinear adjoint estimate has an expectation of 0. This corresponds to the ballistic assumption in the truth trajectory as discussed previously. The estimator only deviates from this ballistic trajectory in presence of error. This can include measurement error, a priori state error, and dynamic mismodeling. The first two errors are quantifiable with the given information, and the final is a deterministic mismodeling. The purpose of the maneuver detection method discussed in the next section is to identify the presence of this mismodeling.

$$\delta\hat{p}_{k-1|k} = \bar{P}^{-1}_{k-1|k-1}\left(\delta\bar{x}_{k-1|k-1} - \delta\hat{x}_{k-1|k}\right) - \tilde{p}_{k-1|k} \tag{22}$$

Finally, we complete the definition of the GL-OCBE with covariance of the state estimates. The measurement epoch covariance is defined in Eq. 23, and the a priori estimate covariance is defined in Eqs. 24 and 25.

$$\hat{P}_{k|k} = \left(I - L_k\tilde{H}_k\right)\bar{P}_{k|k-1}\left(I - L_k\tilde{H}_k\right)^T + L_kR_kL_k^T \tag{23}$$

$$\begin{aligned}
\hat{P}_{k-1|k} =& \mathcal{I}_{k-1}\bar{P}_{k-1|k-1}\mathcal{I}_{k-1}^T + L_{k-1}\left(R_k + \tilde{H}_k\bar{P}_{k|k-1}\tilde{H}_k^T\right)L_{k-1}^T \\
&+ \mathcal{I}_{k-1}\bar{P}_{k-1|k-1}\Phi_{pp}^{-1}\left(E\left[\vec{v}_p(t_k|t_{k-1})\vec{v}_p(t_k|t_{k-1})^T\right]\right)\Phi_{pp}^{-T}\bar{P}_{k-1|k-1}\mathcal{I}_{k-1}^T \\
&- \mathcal{I}_{k-1}\bar{P}_{k-1|k-1}\left[\Phi_{xx} + \mathcal{P}_{k|k-1}\Phi_{px}\right]^T\tilde{H}_k^TL_{k-1}^T - L_{k-1}\tilde{H}_k\left[\Phi_{xx} + \mathcal{P}_{k|k-1}\Phi_{px}\right]\bar{P}_{k-1|k-1}\mathcal{I}_{k-1}^T \\
&- \mathcal{I}_{k-1}\bar{P}_{k-1|k-1}\Phi_{pp}^{-1}\left(E\left[\vec{v}_p(t_k|t_{k-1})\vec{v}_p(t_k|t_{k-1})^T\right]\right)\mathcal{P}_{k|k-1}\tilde{H}_k^TL_{k-1}^T \\
&- \mathcal{I}_{k-1}\bar{P}_{k-1|k-1}\Phi_{pp}^{-1}\left(E\left[\vec{v}_p(t_k|t_{k-1})\vec{v}_x(t_k|t_{k-1})^T\right)\right]\tilde{H}_k^TL_{k-1}^T \\
&- L_{k-1}\tilde{H}_k\mathcal{P}_{k|k-1}\left(E\left[\vec{v}_p(t_k|t_{k-1})\vec{v}_p(t_k|t_{k-1})^T\right]\right)\Phi_{pp}^{-T}\bar{P}_{k-1|k-1}\mathcal{I}_{k-1}^T \\
&- L_{k-1}\tilde{H}_k\left(E\left[\vec{v}_x(t_k|t_{k-1})\vec{v}_p(t_k|t_{k-1})^T\right]\right)\Phi_{pp}^{-T}\bar{P}_{k-1|k-1}\mathcal{I}_{k-1}^T
\end{aligned} \tag{24}$$

$$E\left[\vec{v}_p(t_k|t_{k-1})\vec{v}_p(t_k|t_{k-1})^T\right] = \int_{t_{k-1}}^{t_k} \Phi_{px}(t_k,\tau)B(\tau)\tilde{Q}(\tau)B(\tau)^T\Phi_{px}(t_k,\tau)^T d\tau \tag{25}$$

$$E\left[\vec{v}_x(t_k|t_{k-1})\vec{v}_p(t_k|t_{k-1})^T\right] = \int_{t_{k-1}}^{t_k} \Phi_{xx}(t_k,\tau)B(\tau)\tilde{Q}(\tau)B(\tau)^T\Phi_{px}(t_k,\tau)^T d\tau$$

As might be expected, the form of the measurement epoch covariance is incredibly similar to the Kalman estimate covariance. Both covariances when reduced for a ballistic nominal trajectory are equivalent to the Kalman uncertainties thus extending the equivalence to uncertainties as well as estimates. It should be noted that Eq. 25 may be reformulated into a form that is more practical for numerical implementation using properties of the STM, but that will not be addressed in this discussion.

These equations fully define the GL-OCBE. Generally, the GL-OCBE is initialized about a ballistic trajectory, and then iterated until the OCBE necessary conditions are satisfied, thus solving the nonlinear estimation problem. The resulting uncertainties are appropriate linear uncertainties in the nonlinear estimates. The optimal control policy may be obtained via Eq. 5. This is far more meaningful piece of information than the adjoint, and it will form the basis of the maneuver detection method discussed in the follwoing section.

3. ADAPTIVE ESTIMATION USING MANEUVER DETECTION

The quantity that makes the OCBE unique is it control estimate. These control estimates are reconstructions of dynamic mismodeling, and they may also be used to determine whether the mismodeling is statistically significant. We call this process maneuver detection. The term maneuver refers to any type of dynamic mismodeling - natural or actuated. This section includes an overview of the OCBE maneuver detection process, and how that process may be used to automate the algorithm. The resulting algorithm is called the Adaptive OCBE.

3.1. Maneuver Detection and Reconstruction in the OCBE

The OCBE maneuver detection method is based on the control distance metrics method developed by Holzinger, Scheeres, and Alfriend [10]. They defined a single metric based on estimated optimal control policies, and then used statistical methods to determine whether the estimated controls were statistically significant. For the OCBE, we use three metrics: 1) the OCBE control distance metric (Eq. 26), 2) the OCBE measurement distance metric (Eq. 27), and 3) the OCBE a priori state distance metric (Eq. 28). These three metrics form the three terms of the OCBE cost function, thus they are physically significant to this problem. By separating the metrics we are also able to understand and independently analyze the three possible sources of error in the estimation problem.

$$D_C(\hat{u}(t)) = \int_{t_{k-1}}^{t_k} \frac{1}{2}\left(\vec{u}(\tau)-\bar{u}(\tau)\right)^T \tilde{Q}(\tau)^{-1}\left(\vec{u}(\tau)-\bar{u}(\tau)\right) d\tau \tag{26}$$

$$D_M(\hat{x}_{k|k}) = \frac{1}{2}\left(\vec{Y}_k - h(t_k,\hat{x}_{k|k})\right)^T R_k^{-1}\left(\vec{Y}_k - h(t_k,\hat{x}_{k|k})\right) \tag{27}$$

$$D_A(\hat{x}_{k-1|k}) = \frac{1}{2}\left(\bar{x}_{k-1|k-1}-\hat{x}_{k-1|k}\right)^T \bar{P}_{k-1|k-1}^{-1}\left(\bar{x}_{k-1|k-1}-\hat{x}_{k-1|k}\right) \tag{28}$$

As mentioned, these metrics have a quadratic-Gaussian form, which is very similar to a χ^2 distribution. If we put the metrics in the form of Eq. 29 (where $\vec{z}$ is a zero mean Gaussian random vector with covariance $P_z^{-1/2}M_zP_z^{-1/2}$), then we can reformulate the metric into a χ^2 random variable via Pearson's approximation [10].

$$D_Z = \vec{z}^T M_z \vec{z} \tag{29}$$

This reformulation via Pearson's approximation is defined in Eq. 30 where λ_j are the eigenvectors of the matrix $P_z^{-1/2}M_zP_z^{-1/2}$, and ν is number of degrees of freedom for the χ^2 random variable.

$$D_z \approx \frac{\theta_3}{\theta_2}\chi_\nu^2 + \left(\theta_1 - \frac{\theta_2^2}{\theta_3}\right) \tag{30}$$
$$\theta_s = \textstyle\sum_{j=1}^r \lambda_j^s, \quad \nu = \frac{\theta_2^3}{\theta_3^2}$$

The process of converting our metrics to the form of Eq. 29, requires the substitution of the GL-OCBE estimates, and the computation of the P_z covariances. This process is straightforward, thus we will leave it out of this discussion.

To perform maneuver detection the user needs to define a maneuver threshold percentile. This percentile is then converted to the relevant χ^2_ν value. With this definition it is possible to have a fractional value for ν. In this case the user should interpolate between integer values for ν to find the appropriate χ^2_ν. Once this value has been obtained it can be mapped into metric space via Eq. 30 to form the metric threshold. If the calculated metric exceeds this threshold, then the user can conclude that some mismodeling is present in the system, thus the estimated control profile is statistically significant. Once the maneuver has been detected, the assumed dynamic uncertainty ($\tilde{Q}(t)$) should be adjusted until the maneuver is no longer detected. Doing this fully compensates for the maneuver. In the next section a method for automatically adjusting the assumed dynamic uncertainty when a maneuver is detected is discussed.

3.2. The Adaptive OCBE

The maneuver detection results tell us whether our system is properly tuned to the errors within this system. Assuming measurement and a priori state uncertainties are properly tuned, the remaining source of error is dynamical mismodeling. Increasing the assumed dynamic uncertainty tells the filter to anticipate larger dynamic mismodeling, and it compensates for this perceived increase in error by inflating the state covariances. The assumed dynamic uncertainty should be adjusted until the maneuver is no longer detected, thus indicating it has been addressed properly through compensating uncertainty. This process, when done by hand is cumbersome and costly in terms of time, thus it is infeasible to accomplish with a human in the loop for data sets on the scale of SSA problems. The Adaptive OCBE addresses this issue by automating the selection of the assumed dynamic uncertainty.

This algorithm automatically selects an assumed dynamic uncertainty under the criterion that the mean of the metric's distribution and the calculated metric are equal to one another, since this is our best estimate of what the metric should be. The mean of a random variable of the form in Eq. 29 is defined in Eq. 31.

$$\mu_z = \mathrm{Tr}\left[M_z P_z\right] \tag{31}$$

To simplify this problem we also reduce the dimensionality of the problem by specifying the assumed dynamic uncertainty as a scalar variable (σ_Q) multiplied by a unit correcting factor (a) on the diagonals of a matrix (Eq. 32). We will refer to σ_Q as the assumed dynamic standard deviation.

$$\tilde{Q}(t) = a\sigma_Q^2 I_{m\times m} \tag{32}$$

All three OCBE metrics and their means are functions of the assumed dynamic uncertainty, thus we must select σ_Q such that the metric and mean intersect. In practice a solution always exist providing a maneuver was detected. However if no maneuver was detected, then it is possible for the mean and metric to have no intersection as functions of σ_Q. For these cases we define a value called the dynamic noise floor ($\sigma_{Q,NF}$). This is low value that defines the minimum level dynamic uncertainty that the user cares about - any mismodeling below this level is considered negligible. When there is no detected maneuver or there is no solution that equates the metric and its mean, then we default to this value. Finding the proper σ_Q when not defaulting to the noise floor is a nonlinear root finder problem. Any suitable method may be used. The authors have have used numerical Newton-Secant and Newton-Raphson methods with success.

How a maneuver is defined between the three metrics is up to the user. One metric or more may be relied upon at any given time. In the analysis that follows a maneuver is detected when all three metrics exceed their thresholds simultaneously (this helps to eliminate false detections). A delay mechanism may also be implemented. The delay waits for a preset number of successive maneuvers to be detected. When that number is reached the algorithm automatically returns to the original detection, adjusts the assumed dynamic standard deviation appropriately and continues onward. This method helps to distinguish between a single outlier in the data versus deterministic mismodeling, which affects many estimates down the chain, thus it will be detected repeatedly if not addressed properly. While this results in a delay for a maneuver to be addressed, the detection still happens in real time.

These processes are automated, thus it takes the human out of the loop. In the following section we will demonstrate the effectiveness of this algorithm applying it to a sample GEO spacecraft tracking problem.

4. SIMULATIONS AND RESULTS

In this sample tracking scenario, a spacecraft in GEO is being observed via a ground station with non-cooperative range (10 m Gaussian uncertainty) and azimuth and elevation angle (1 arcsecond Gaussian uncertainty) observations. The spacecraft is observed for two hours each night (observations taken every 100 seconds) over the course of fifteen days. Unknown to the estimator, the spacecraft executes stationkeeping maneuvers periodically to account for latitude (North-South [NS] maneuver) and longitude (East-West [EW] maneuver) deviations from the nominal geosynchronous orbit at a longitude of 60 degrees. The true dynamical model includes two body gravity, oblateness effects, solar radiation pressure (with area-to-mass ratio of 0.024), third body effects (sun and moon), and the actuated maneuvers. More perturbations may be included, but they do not effect the results unless they are mismodeled.

The actuated maneuvers are designed as low thrust events that last 4 hours. They initiate when a latitude or longitude nominal deviation barrier is crossed (0.05 degrees latitude and 0.1 degrees longitude), and conclude 4 hours later when the latitude or longitude has been reset to the nominal value. The maneuvers are decoupled such that latitude maneuvers do not influence longitude and vice versa.The spacecraft starts with an initial 0.25 degree deviation from nominal in latitude, a 0.2 degree deviation from nominal in longitude, and no deviation from nominal in radius.

To start the simulation the true trajectory is mismodeled on the order of 1 km in position and 1 m/s in velocity. The GL-OCBE is then iterated until convergence to solve the nonlinear necessary conditions with each new measurement, and uncertainties are calculated using the GL-OCBE linearizations. Detected maneuvers are defined as when all three metrics exceed their respective thresholds simultaneously. The delay algorithm requires two successive maneuvers be detected before addressing it with an adjusted dynamic uncertainty. This helps to differentiate between measurement outliers and true maneuvers so that the state uncertainty does not become artificially over inflated. This analysis uses a 99% threshold percentile for maneuver detection. When successive maneuvers are detected, an assumed dynamic standard deviation is chosen to ensure the mean of the control metric is equal to the calculated metric. The dynamic noise floor is set to $\sigma_{Q,NF} = 10^{-10}$ m/s^2.

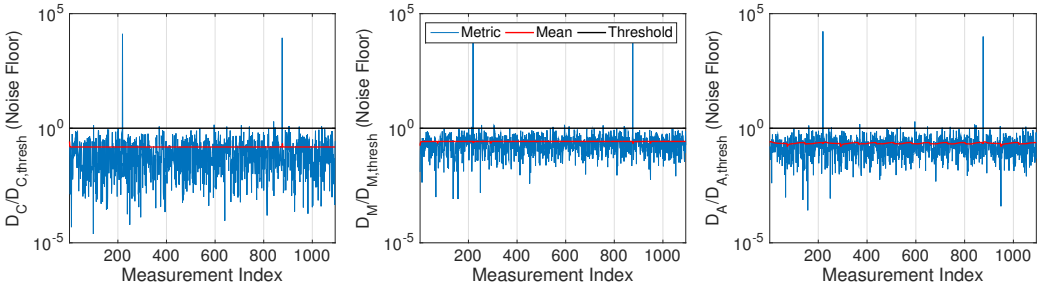

Figure 1: Distance metric to metric threshold ratio before applying adaptive algorithm.

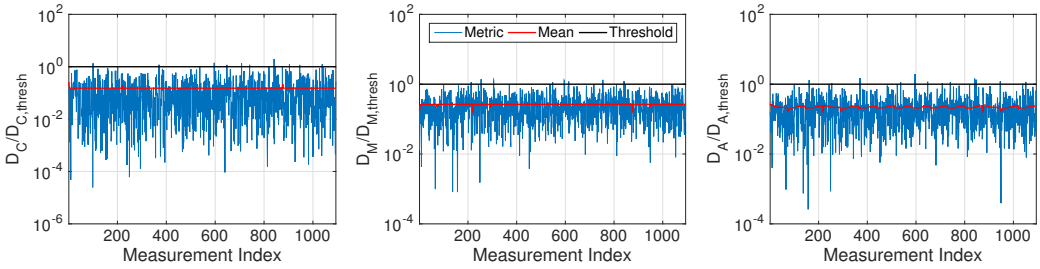

Figure 2: Distance metric to metric threshold ratio after applying adaptive algorithm.

Figure 1 shows the metric-threshold ratio for all three metrics. This is defined as the ratio of the distance metric to the distance metric threshold, thus anything exceeding one is a detected maneuver for that specific metric. For all three metrics we see the expected dispersion about the mean of the distribution with approximately one percent of the metrics exceeding the threshold (1.19% for the control metric, 1.10% for the measurement metric, and 1.37% for the a priori metric). In total there are 4 epochs where the three metrics simultaneously exceed their thresholds.

However, when implementing the delay mechanism only two of these epochs stand out as true detected maneuvers. These correlate to the two true maneuvers. This tells us that the algorithm was able to successfully identify the only true maneuvers without any false detections in 1,094 observations.

While the previous metrics show maneuvers with respect to the noise floor, Fig. 2. Shows maneuvers with respect to the adaptive assumed dynamic uncertainty. These results confirm the adaptive algorithm is working properly since the two maneuver detection events are removed. This indicates that the two detected maneuvers have been addressed with a proper level of dynamic uncertainty. For each metric some events still exceed the threshold, but these are because they were identified as being outliers rather than deterministic events via the combination of the three combined metrics and application of the delay mechanism.

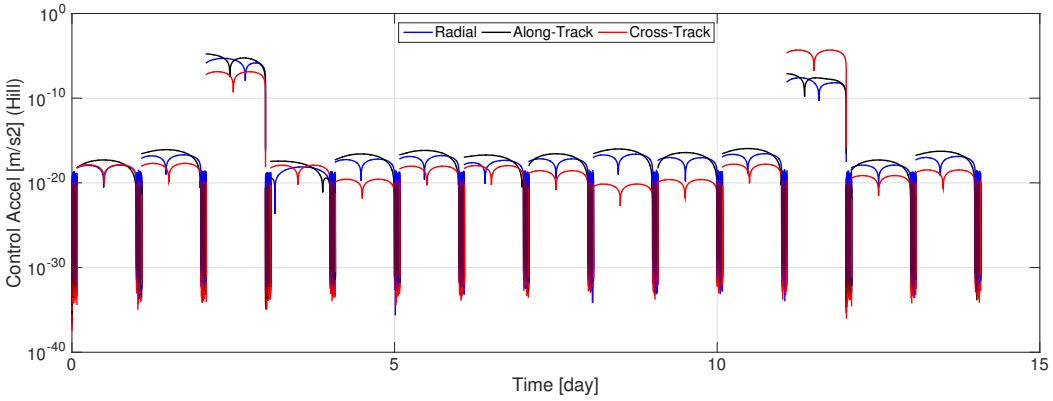

Figure 3: Magnitude of estimated controls in Hill frame.

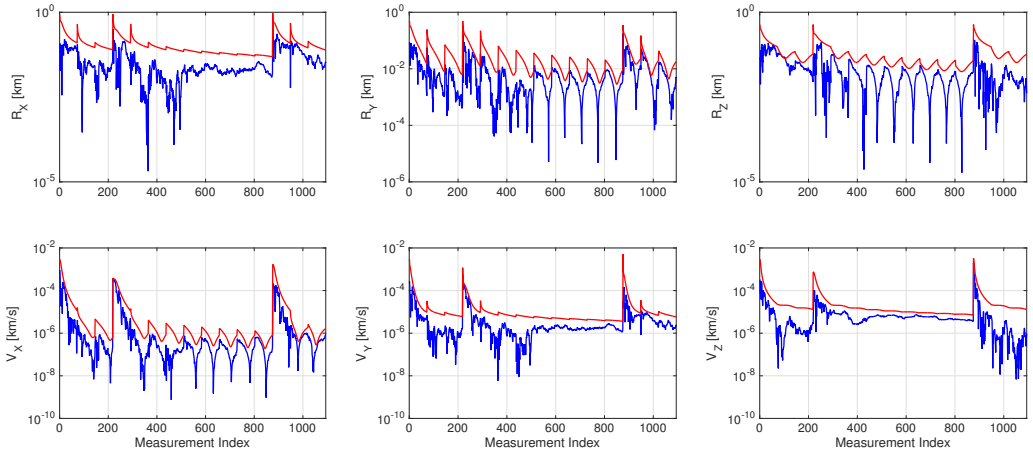

Figure 4: Cartesian state estimate deviations from truth against measurement index with a 3-σ envelope (red).

To this point it is clear that we successfully detected the presence of the only two maneuvers with no false detections. Our next step is to reconstruct these maneuvers to provide information on them. The first piece of information are the control estimates we obtained from the estimator. The magnitude of these controls in the Hill frame are shown in Fig. 3. The identified maneuvers clearly stick out in this plot with the rest of the estimated control being effectively zero. The first maneuver is heavily biased toward in plane accelerations with the radial and along-track directions approximately 2-3 orders of magnitude larger than the cross-track acceleration. This indicates that the maneuver is an EW maneuver. Similarly, the second maneuver is heavily biased toward the cross-track direction, which indicates that this is a NS maneuver. Additionally, we may use the metrics themselves to inform our reconstruction of the maneuvers. Because the maneuvers are one time events it becomes evident that they represent some non-natural process.

This reinforces the hypothesis that the mismodeling is related to an actuated maneuver. We may also characterize the maneuvers based on these estimates as 0.525 m/s and 2.535 m/s maneuvers compared to the true values of 16.8652 m/s and 7.6552 m/s, respectively. Because these estimates are based on optimal controls they provide a lower bound on the true maneuver, but also give an order of magnitude estimate.

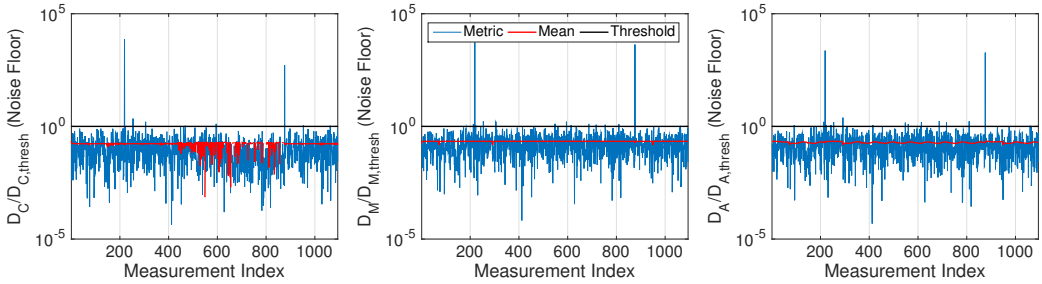

Figure 5: Distance metric to metric threshold ratio before applying adaptive algorithm with angles-only observation.

Finally, the results displayed in Fig. 4 show the level of tracking obtained with the OCBE. It is clear that the estimator maintains tracking of the spacecraft throughout both maneuvers and across all observation gaps. Tracking is attained on the 10 m level, which reflects the uncertainty in the measurements.

It should be noted that similar maneuver detection results are obtained with angles only observation. Fig. 5 shows the metric-to-threshold ratio results when the algorithm is run with angles only observation. Just as with the previous simulation, the only two events that are detected as maneuvers are the two true events. Tracking is not as good with fewer observations giving levels of approximately 1 km in position, rather than the 10 m level achieved with range. There are also observability issues that pop up as would be the case with a Kalman Filter. This does not prevent a solution, it just leads to tracking falling out of the 3-σ envelope more frequently.

This simulation shows the Adaptive OCBE's ability to automatically track an object with mismodeled dynamics as well as detect and reconstruct that mismodeling. The algorithm correctly identified both maneuvers with no false detections in the 1,094 measurements processed. Even with fewer observation types the detection aspect of the work does not suffer, though tracking uncertainty increases due to a decrease in the amount of information.

5. CONCLUSIONS AND FUTURE WORK

This paper addresses the problem of estimation is dynamically mismodeled systems in an automated fashion while detecting and reconstructing the mismodeling. The Adaptive OCBE is presented as an algorithm that addresses this problem. It is a state estimator that accounts for dynamic mismodeling by reconstructing mismodeled dynamics via estimated optimal control policies. These control policies may also be used in a maneuver detection algorithm that accurately identifies when mismodeled dynamics are present. This maneuver detection algorithm is then used to automate the OCBE such that the algorithm detects mismodeling and automatically compensates for it without a human in loop. A sample tracking simulation demonstrated the effectiveness of this algorithm. The Adaptive OCBE accurately detected two maneuvers without any false detections in the entire 15-day observation arc, and it provided enough information to allow us to approximate the size of the maneuver and the type of maneuver. It accomplished all of this with in a completely automated fashion.

Looking forward, this estimator can be advanced for SSA application by considering multi-target tracking with uncorrelated observations. The algorithm is already designed to work an arbitrary orbit-observer setup, so by expanding it to deal with n targets the method would be readily implementable to all types of SSA surveys.

ACKNOWLEDGEMENTS

This work was supported by a NASA Office of the Chief Technologist's Space Technology Research Fellowship. DJS was supported in part by grant FA9550-11-1-0188 from AFOSR.

References

[1] J. Ahmed, V. T. Coppola, and D. S. Bernstein. Asymptotic tracking of spacecraft attitude motion with inertia matrix identification. *Journal of Guidance, Control, and Dynamics*, 21(5):684–691, 1998.

[2] Y. Bar-Shalom and K. Birmiwal. Variable dimension filter for maneuvering target tracking. *Transactions on Aerospace and Electronic Systems*, 18(5):621–629, 1982.

[3] R. Brincker, L. Zhang, and P. Andersen. Modal identification of output-only systems using frequency domain decomposition. *Smart Materials and Structures*, 10(3):441–445, 2001.

[4] Y. T. Chan, A. G. C. Hu, and J. B. Plant. A kalman filter based tracking scheme with input estimation. *Transactions on Aerospace and Electronic Systems*, 15(2):237–244, 1979.

[5] J. Chandrasekar and D. S. Bernstein. Position control using acceleration-based identification and feedback with unknown measurement bias. *Journal of Dynamic Systems, Measurement, and Control*, 130(1), 2007.

[6] Z. J. Folcik, P. J. Cefola, and R. I. Abbot. Geo maneuver detection for space situational awareness. *Advances in Astronautical Sciences*, 129:1058–1074, 2007.

[7] G. M. Goff, J. T. Black, and J. A. Beck. Orbit estimation of a continuously thrusting spacecraft using variable dimension filters. In *AIAA Guidance, Navigation, and Control Conference*, January 2015.

[8] P. D. Hanlon and P. S. Maybeck. Characterization of kalman filter residuals in the presence of mismodeling. *IEEE Transactions on Aerospace and Electronic Systems*, 36(1):114–131, 2000.

[9] K. Hill. Maneuver detection and estimation with optical tracklets. In *Advanced Maui Optical and Space Surveillance Technologies Conference*, September 2014.

[10] M. J. Holzinger, D. J. Scheeres, and K. T. Alfriend. Object correlation, maneuver detection, and characterization using control distance metrics. *J. Guidance, Control, and Dynamics*, 35(4):1312–1325, 2012.

[11] A. H. Jazwinski. *Stochastic Processes and Filtering Theory*. Elsevier Academic Press, 1970.

[12] D. F. Lawden. *Optimal Trajectories for Space Navigation*. Butterworths Mathematical Texts, 1963.

[13] D. F. Lawden. *Analytical Methods of Optimization*. Dover Publications Inc., 1975.

[14] S. Lee and I. Hwang. Interacting multiple model estimation for spacecraft maneuver detection and characterization. In *AIAA Guidance, Navigation, and Control Conference*, January 2015.

[15] S. Lemmens and H. Krag. Two-line-elements-based maneuver detection methods for satellites in low earth orbit. *Journal of Guidance and Control*, 2014.

[16] X. R. Li and V. P. Jilkov. Survey of maneuvering target tracking. part i: Dynamic models. *IEEE Transactions on Aerospace and Electronic Systems*, 39(4):1333–1364, 2005.

[17] L. Ljung. *System Identification:Theory for the User*. Prentice Hall, 2nd edition, 1999.

[18] D.P. Lubey and D.J. Scheeres. Supplementing State and Dynamics Estimation with Information from Optimal Control Policies. In *17th International Conference on Information Fusion*, July 2014.

[19] D.P. Lubey and D.J. Scheeres. Automated State and Dynamics Estimation in Dynamically Mismodeled Systems with Information from Optimal Control Policies. In *18th International Conference on Information Fusion*, July 2015.

[20] R. P. Patera. Space event detection method. *Journal of Spacecraft and Rockets*, 45(3):554–559, 2008.

[21] B. D. Tapley, B. E. Schutz, and G. H. Born. *Statistical Orbit Determination*. Elsevier Academic Press, 1st edition, 2004.

[22] D. Wang and A. Haldar. System identification with limited observations and without input. *Journal of Engineering Mechanics*, 123(5):504–511, 1997.